2006 IEEE International Conference on
Systems, Man, and Cybernetics
October 8-11, 2006, Taipei, Taiwan

The Human-in-the-loop Design Approach to the Longitudinal Automation System for the Intelligent Vehicle, TAIWAN *i*TS-1

Hsin-Han Chiang, Jau-Woei Perng, Bing-Fei Wu, Shinq-Jen Wu, and Tsu-Tian Lee

***Abstract*—This paper presents the integration design and implementation of a longitudinal automation system with the interaction of human-in-the-loop (HITL). The proposed system has a hierarchical structure composed and consists of an adaptive sensory processor, a supervisory control and a regulation control. The adaptive sensory processor routes the information from on-board sensors to avoid missing detection of the vehicle ahead. Based on the recognized measurement from the adaptive sensory processor, the supervisory control determines the desired velocity for the vehicle so as to maintain safety and smooth operation in different modes. The regulation control utilizes soft-computing technique and drives the throttle action to execute the desired velocity commanded from the supervisory control. The feasible sensory distance is within 40 m, and the according driving velocity can achieve 100 km/h upward. The challenge in low velocity operation can also be handled by the regulation control against gear changes and torque converter. Among experimental tests under various kinds of traffic flows, the system validness is exhibited and also the preferable comfort is achieved through the examination of international standard ISO 2631.**

I. Introduction

Vehicle automations are currently being introduced into the assistance to relieve human drivers from undesired routines of driving task. Since many studies have shown that over 90 percent of highway accidents are occurred due to driver -related errors, the main initiative is to improve safety of the automation system interacted with the human driver. As to the vehicle longitudinal automation control, some famous practical works [1-3] introduce the features like adaptive cruise control (ACC). The more understandings of the automation of vehicle longitudinal control task are provided in [4]. Besides, to increase more capability being with human drivers, the conception of human-in-the-loop (HITL) needs to be more considered into the system design.

The safety consideration into the vehicle longitudinal automation is the safety headway distance adjustment to avoid the collision with the vehicle ahead. To accommodate the automation system to different driving conditions, the corresponding operation modes and the automatic transition frame should be developed. There is no initial demand for road environment, and also for the action of the human driver which can be viewed as a disturbance to the automation system. It is essential to consider the adequate stability and robustness into the controlling design. Moreover, drivers' comfort is also the most important initiative counted for automation design.

H. H. Chiang, J. W. Perng, B. F. Wu, and T. T. Lee are with National Chiao-Tung University, Hsinchu, 300, Taiwan, R. O. C. (authors to provide phone: 886-3-5712121-54346; fax: 886-3-5729749; e-mail: hsinhan.ece90g @nctu.edu.tw; jwperng@cn.nctu.edu.tw; bwu@cssp.cn.nctu.edu.tw; ttlee@ cn.nctu.edu.tw)

S. J. Wu is with Da-Yeh University, Changhwa, Taiwan, R. O. C. (e-mail: jen@mail.dyu.edu.tw)

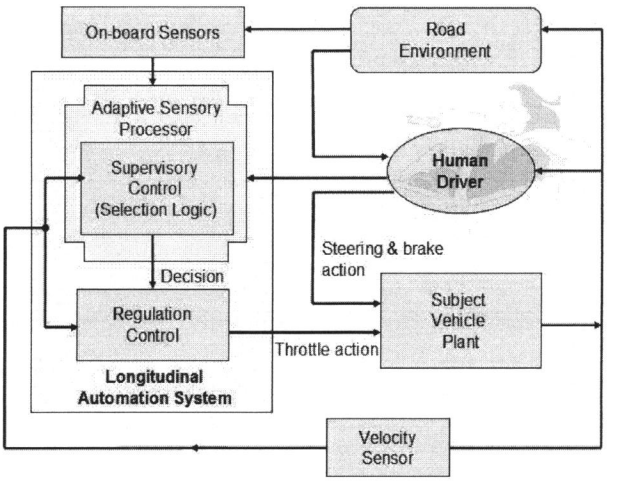

Fig. 1. Overall structure of the human-in-the-loop longitudinal automation system.

This paper proposes the longitudinal automation system, which is implemented on a real vehicle named TAIWAN *i*TS-1, with the interaction of the human driver. The special modifications to the automation system are to ensure safety and smooth operation with workload reduction for the human driver. Finally, experimental results in real road environments document the performance of the overall system integration extended to the capability of HITL design.

II. System Configuration and Objectives

As illustrated in Fig. 1, the road environment mainly refers to the longitudinal direction in front of the subject vehicle, and the on-board sensors include laser radar and angle sensor of the steering wheel (SW). The adaptive sensory processor deals with measurements from radar according to the action of human driver and the velocity of the vehicle. Based on the recognized data, the supervisory control makes the decision of operation modes and desired velocity command to the regulation control for the execution of velocity tracking. The throttle pedal is driven by the longitudinal automation system to achieve the controlling objective. Although the brake pedal can be automated in our mechanism, in this work it is not used

TABLE I
CRITICAL THRESHOLD OF COMFORT IN ISO 2631 STANDARD

No discomfort (~ 0.315 m/s^2)
A little discomfort (0.315 ~ 0.63 m/s^2)
Somewhat discomfort (0.5 ~ 1 m/s^2)
Discomfort (0.8 ~ 1.6 m/s^2)
Extremely discomfort (1.25 ~ 2.5 m/s^2)
Very discomfort (2 m/s^2 ~)

and reserved for the human driver to take the awareness of emergency.

As far as the longitudinal automation convinced to the human driver is concerned, the controlling operation for the subject vehicle comprises the velocity tracking cruise mode and automatic vehicle following mode. In the velocity tracking cruise mode, the objective is to control the subject vehicle to track any desired velocity commanded from the human driver. At the time of the detection from the preceding vehicle, the automation system will automatically switch to the automatic vehicle following mode. The objective of this mode is to make sure of safety headway distance maintaining for the subject vehicle without the need of vehicle-to-vehicle (v-v) communication. In addition, the automation system will automatically switch back to the velocity tracking cruise mode if there is no vehicle detection in the front.

In these both operation modes, the ride comfort of the human driver or passengers is considered into the automation design. As the comfort analysis concern, the international standard ISO 2631-1:1997 [5], which defines the means to evaluate vibration with respect to human responses, is employed to examine the ride quality of the proposed longitudinal automation system. This standard specifies direction and location of measurements, equipment to be used, duration of measurements and frequency weighting, as well as methods of assessment of measurement and evaluation of weight root-mean-square (r-m-s) acceleration in meters per second squared (m/s^2). The index of this standard is determined by the frequency-weighted acceleration which can be calculated by using the expression as

$$a_w = \left[\sum_i (W_i a_i)^2 \right]^{1/2}, \tag{1}$$

where a_w denotes frequency-weighted acceleration, W_i denotes the weighting factor of interesting axes of body, and a_i denotes the r-m-s acceleration for the i-th one-third octave band.

The comfort analysis is assessed by checking that a_w over sampled horizon does not reach a critical threshold value, as depicted in Table I. As to the longitudinal automation design, the motion which performs in the longitudinal axis is the interest to be examined for ride comfort of the subject vehicle.

The following section describes the designing approach for the longitudinal automation system to be assured that the safety and comfort requirements can be both achieved.

III. LONGITUDINAL AUTOMATION SYSTEM DESIGN

In this section, the three components of the proposed vehicle longitudinal automation system are introduced, respectively.

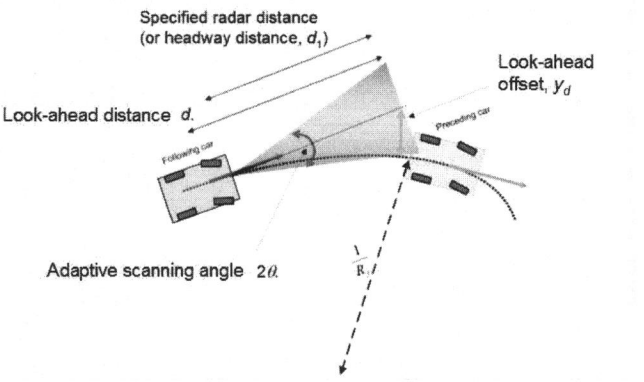

Fig. 2. Illustration of the vehicle following scenario on curved roads.

A. Adaptive Sensory Processor

As illustrated in Fig. 2, the preceding vehicle can not be detected by the laser radar in front of the following vehicle if the scanning beam is too narrow. This fact might bring the emergency due to drastic acceleration action of the system. Nevertheless, if the scanning beam is too broad, some unexpected objects which are neighbor with the road will be detected. Therefore, it is necessary to design the adaptive sensory scheme such that the preceding vehicle can be correctly detected even if on the curved roads.

By considering the turning behavior of the vehicle, a linear bike model of lateral dynamics from steering angle δ_f to lateral velocity v_y and yaw rate r is employed as

$$\begin{bmatrix} \dot{v}_y \\ \dot{r} \end{bmatrix} = A \begin{bmatrix} v_y \\ r \end{bmatrix} + B\delta_f \tag{2}$$

where

$$A = \begin{bmatrix} \dfrac{-(C_f + C_r)}{mV} & -V + \dfrac{-aC_f + bC_r}{mV} \\ \dfrac{-aC_f + bC_r}{I_z V} & \dfrac{-(a^2 C_f + b^2 C_r)}{I_z V} \end{bmatrix}, \quad B = \begin{bmatrix} \dfrac{C_f}{m} \\ \dfrac{aC_f}{I_z} \end{bmatrix},$$

a and b denote the distances from the front and rear axles to the center of gravity (CG) of the vehicle, m denotes the total mass of the vehicle, V denotes the forward velocity, I_z denotes the yaw moment of inertia, and C_f and C_r denote the total cornering stiffness of the front and rear tires, respectively.

In addition, to detect the existence of the preceding vehicle, the look-ahead information of the subject vehicle must be considered. The dynamics of the point at a look-ahead distance of the moving vehicle can be described as

$$\dot{y}_d = V\varepsilon_d - v_y - rd \tag{3}$$

$$\dot{\varepsilon}_d = V / R_f - r \tag{4}$$

where y_d and ε_d denote the lateral offset from the centerline and the angle between tangent to the road and the vehicle at a look-ahead distance d, and R_f denotes the road curvature.

Note that here the road curvature is restricted to be constant for the assumption of the steady-state analysis. The reason is that the vehicle will not reach a steady-state condition while traveling a road with varying curvatures, and then the static relation is difficulty to be investigated. As shown in Fig. 2, the subject vehicle (or called following vehicle) and the preceding vehicle both travel a curve with a constant

TABLE II
(δ_f, θ) WITH VARYING VELOCITIES AND RADIUS OF CURVED ROADS

V \ R_f	200 m	300 m	400 m	500 m
40 km/h	(19.6, 6.9)	(14.5, 5.1)	(10.9, 3.8)	(8.7, 3.1)
60 km/h	(23.9, 9.2)	(15.5, 6.1)	(11.6, 4.6)	(9.3, 3.7)
80 km/h	(25.1, 11.9)	(16.8, 7.9)	(12.6, 5.9)	(10.1, 4.7)
100 km/h	(27.6, 16.6)	(18.4, 11.1)	(13.8, 8.3)	(11.1, 6.6)

Unit: degree

curvature $1/R_f$. By considering a steady-state motion that the subject vehicle tracks the curved road perfectly at a constant velocity, the variations of the vehicle lateral dynamics (2) and look-ahead dynamics (3) and (4) can be set to zero, i.e., $\dot{v}_y = \dot{r} = \dot{y}_d = \dot{\varepsilon}_d = 0$. In the following, the subscript of *ss* denotes the value at steady-state condition. Through direction calculation, the steady-state steering angle can be obtained as

$$\delta_{fss} = \frac{1}{R_f}(a+b-\frac{mV^2(aC_f - bC_r)}{(a+b)C_fC_r}) \tag{5}$$

The steady-state look-ahead lateral offset can be adopted as

$$y_{dss} = h_{ss} - R_f \tag{6}$$

where $h_{ss} = \sqrt{R_f^2 + d^2 + 2R_f d(-v_{yss}/V)}$.

Besides, at steady-state the lateral dynamics (2) can be presented as

$$A\begin{bmatrix} v_{yss} \\ r_{ss} \end{bmatrix} = -B\delta_{fss} \tag{7}$$

and this holds if and only if

$$v_{yss} = -r_{ss}T \tag{8}$$

where $T = b + amV^2/(a+b)C_r$.

Note that the fixed values of the yaw rate can be obtained by

$$r_{ss}=V/R_f \tag{9}$$

which is assumed in the steady-state turning.

By substituting (8) and (9) into (6), the look-ahead steady-state look-ahead lateral offset can be rewritten as

$$y_{dss} = \sqrt{R_f^2 + d^2 + 2dT} - R_f \tag{10}$$

From (5) and (10), one obtains

$$\frac{y_{dss}}{\delta_{fss}} = \frac{R_f\sqrt{R_f^2 + d^2 + 2dT} - R_f^2}{(a+b-mV^2(aC_f - bC_r)/(a+b)C_fC_r)} \tag{11}$$

It is reasonably to assume

$$|d^2 + 2dT| / R_f^2 << 1 \tag{12}$$

and the following approximation via Taylor's expansion can be obtained as

$$\sqrt{R_f^2 + d^2 + 2dT} = R_f + \frac{d^2 + 2dT}{2R_f} \tag{13}$$

Through (13), the relation (11) becomes

$$\frac{y_{dss}}{\delta_{fss}} = \frac{d^2 + 2dT}{2(a+b-V^2P)} \tag{14}$$

where $P = m(aC_f - bC_r)/(a+b)C_fC_r$.

To obtain the relation between the adaptive scanning angle and the steering angle, the following approximation is applied as

$$\tan\theta \cong y_{dss}/d_1 \tag{15}$$

where d_1 denotes the specified distance in the feasible range for laser radar.

By substituting (14) into (15) with the small angle assumption which assumes $\tan\theta \cong \theta$, one can obtain

$$\frac{\theta}{\delta_{fss}} = \frac{d^2 + 2dT}{2d_1(a+b-V^2P)} =: \frac{K_\theta}{d_1} \tag{16}$$

The real input to the vehicle is the steering wheel (SW), and the steering angle can be substituted with the SW angle through a constant ratio [6], i.e., $\delta = i_s\delta_f$, (normally the value of i_s is between 18 and 22 for passenger vehicles). In (16), the resulting feature is that the adaptive ratio between the adaptive scanning angle and the steering angle is independent of the road curvature. It can be observed that the adaptive ratio updates with the vehicle velocity. During the vehicle turning in a higher velocity, the look-ahead lateral offset increases such that the scanning beam is turned more degree with the same direction to the SW. As to less road curvatures, the look-ahead lateral offset decreases such that the scanning angle is turned less degree. Table II depicts this result.

B. Supervisory Control

There are two stages in the supervisory control. In the first stage, the desired acceleration is determined according to the selected operation mode and available feedback signals. In the second stage, the desired acceleration is converted to the desired velocity which is passed into the regulation control.

The velocity tracking cruise mode is to design the desired acceleration such that the subject vehicle can track proper velocities commanded by the driver and avoid feeling discomfort. Define the velocity tracking error as

$$e_V = V - V_{des} \tag{17}$$

and select the sliding surface as

$$S_{CC} = e_V = V - V_{des} \tag{18}$$

To force $S_{CC} = 0$, the control law can be chosen as

$$\dot{S}_{CC} = -K_{CC}S_{CC} \tag{19}$$

where $K_{CC} > 0$ is chosen by the designer.

Equation (19) satisfies the global asymptotically stable requirement and also $S_{CC}\dot{S}_{CC} < 0$. Note that the choice of (19) usually includes the discontinuous sign function, e.g., $sgn(S)$, in typical literatures of sliding mode control (SMC). However, the chattering phenomena will be caused that also brings some unforeseen noise of high frequency. Instead, the continuous function is feasible to be implemented for its simplicity.

By differentiating (18), the desired acceleration will be easily solved with (19). To achieve the requirement of ride comfort, it should keep the acceleration command bounded to the desired one $a_{f\max}$ especially while the initial value of e_V is large. Therefore, the sliding surface in (18) can be modified into

$$S_{CC} = -a_f + a_{f\max}sat(\frac{a_f + e_V}{a_{f\max}}), \tag{20}$$

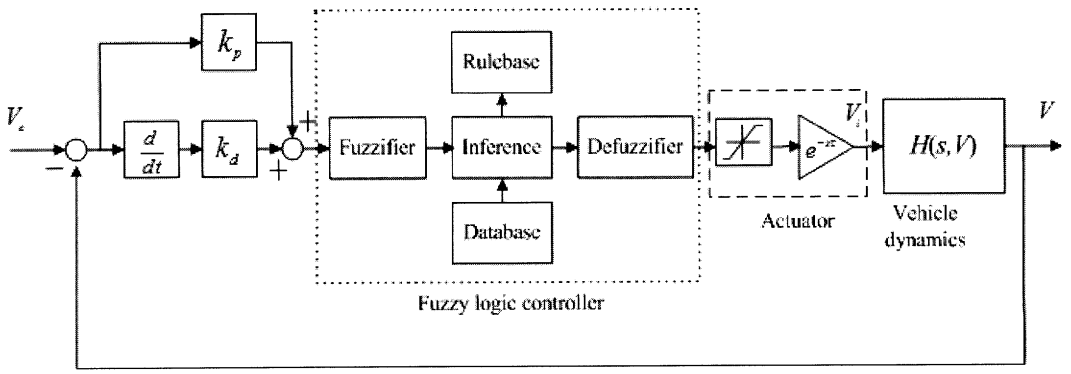

Fig. 3. The block diagram of the closed-loop velocity regulation control.

where a_f is the current acceleration of the following vehicle, and

$$sat(x)=\begin{cases} x, & as\ |x|<1 \\ sign(x), & as\ |x|\geq 1 \end{cases}$$

For the case of $|a_f+e_V|<a_{f\max}$, the sliding surface (20) is identical to the one of (18). The desired acceleration can be solved as

$$a_{f\,des}=\dot{V}_{des}-K_{CC}(V-V_{des}) \tag{21}$$

While $|a_f+e_R|\geq a_{f\max}$, the sliding surface becomes

$$S_{CC}=-a_f\pm a_{f\max}, \tag{22}$$

and the desired acceleration is

$$a_{f\,des}=\frac{-\dot{a}_f}{K_{CC}}\pm a_{f\max} \tag{23}$$

Note that the jerk in (23) can be neglected for the intention of constraint in the desired acceleration, i.e., $a_{f\,des}=\pm a_{f\max}$.

The control law in (21) is rather simple. Since only the velocity of the subject vehicle is required for the velocity tracking mode, implementation of this design is easy and still associated with the consideration of ride comfort.

Continuingly, the objective of the automatic vehicle following mode for headway distance tracking is to design the control law of the desired acceleration. To begin with the development of a sliding surface, the vehicle following dynamics in terms of using the relative distance R are presented as

$$R=X_p-X \tag{24}$$

$$\dot{R}=V_p-V \tag{25}$$

where X and V are the subject vehicle position and velocity, and X_p and V_p are the preceding vehicle position and velocity.

By employing the fixed headway time strategy, the desired following distance law according to the velocity of the subject vehicle can be obtained by

$$R_{des}=\sigma V+L \tag{26}$$

$$\dot{R}_{des}=\sigma a \tag{27}$$

where σ is regarded as the desired headway time, and L can be viewed as a minimum safety distance or typically a vehicle's length.

The error between the desired and relative headway distance is defined as

$$e_R=R-R_{des} \tag{28}$$

and the sliding surface can be designed as

$$S_{VF}=-a_f+a_{f\max}sat(\frac{a_f+e_R}{a_{f\max}}) \tag{29}$$

For the case of $|a_f+e_R|<a_{f\max}$, this sliding surface (29) is obviously stable since $S_{VF}=0$ as $e_R=0$. By choosing the same control law as (19), the desired acceleration can be derived as

$$a_{f\,des}=\frac{1}{\sigma}(K_{VF}S_{VF}+\dot{R}) \tag{30}$$

The result in the case of $|a_f+e_R|\geq a_{f\max}$ is the similar to (23) and the control law $a_{f\,des}=\pm a_{f\max}$ is used instead. In (30), only the headway distance and its change rate are required and the stability is also guaranteed. Note that there is no knowledge of the preceding vehicle existing in (30). Although the states related to the preceding vehicle can be obtained by v-v communication device, it can not be supposed that all other vehicles are equipped.

In the second stage, the conversion from the desired acceleration to the velocity is designed as

$$\dot{V}_{des}=a_{f\,des}-k_t(V-V_{des}) \tag{31}$$

where $k_t>0$ is a damping gain.

As to the selection logic between these two modes, this autonomy scheme can be achieved by adopting the min-operation in the second stage, namely,

$$V_f=\min\{V_{CC},V_{VF}\} \tag{32}$$

Once the preceding vehicle is detected, the final desired velocity for the subject vehicle will be determined by the automatic vehicle following control, i.e., $V_f=V_{VF}$; otherwise, the subject vehicle will be back to the velocity tracking cruise control, i.e., $V_f=V_{CC}$. This approach is intuitive but also easy to implementation.

C. Regulation Control

The objective of the regulation control is to execute the desired velocity commanded from the supervisory control. The vehicle longitudinal dynamics can be described by a set of system composed of various linear and nonlinear subsystems, e.g., engine, automatic transmission in the gear box, brake system, and the rubber tires with respect to roads, etc. Indeed, it is very difficult for control designing based on this complicated model. As to the ill-conditioned and complex model of vehicle longitudinal dynamics, it motivates the employment of fuzzy logic control (FLC) in the regulation control design.

TABLE III
FUZZY RULE BASE OF THE SFLC

D_s	NB	NS	ZO	PS	PB
u	NBu	NSu	ZOu	PSu	PBu

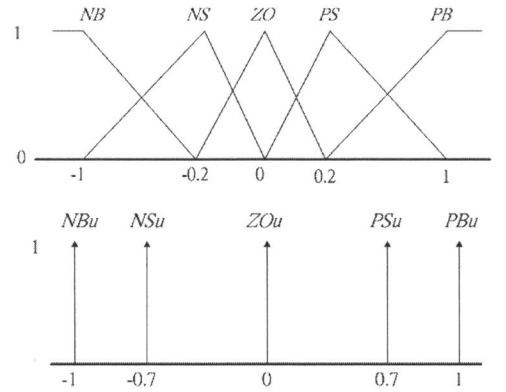

Fig. 4. Membership function of the fuzzy input (up) and the fuzzy output (below).

The block diagram of the regulation control with the vehicle longitudinal dynamics is shown in Fig. 3. The regulation control scheme is composed of a proportion -derivative (PD) controller and a FLC. There is a single control input defined by the error of the commanded and current velocity, i.e., $e = V_c - V$, and the control output is the applied voltage to the throttle motor actuator. The characteristics of the throttle motor actuator can be modeled as one saturation function with a transport delay. $H(s, V)$ presents the dynamics from the derived throttle angle to the vehicle velocity.

This PD-type FLC with a single-input is convincingly representative to the single-input FLC (SFLC) proposed in [7]. For conventional FLC's, the fuzzy rule base is constructed in a two-dimension (2-D) space for using the error and error change phase-plane, i.e., $(e, \dot{e})$. It can be inspected that most 2-D fuzzy rule bases have the so-called skew-symmetric property. One new fuzzy input composed of the error and error change can be presented as

$$D_s = k_d \dot{e} + k_p e \tag{33}$$

Therefore, the 2-D fuzzy rule base of the error and error change phase-plane can be reduced into 1-D space of D_s for SFLC as listed in Table III. Both the ranges of the fuzzy input and output are the same from -1 to 1, and the corresponding membership functions are plotted in Fig. 4, respectively.

In the defuzzication operation, the center of mass (COM) method is applied to calculate the control output

$$u^* = \sum_i^5 \mu_i(D_s) \times u_i \Big/ \sum_i^5 \mu_i(D_s) \tag{34}$$

where μ_i represents the weighting value of each rule i, and u_i is the crisp value of each rule consequence.

There are many advantages for applying this PD-type SFLC. Regardless of the controlled plant dynamics, it requires only one fuzzy input and a 1-D space of fuzzy rule base. Therefore, the number of tuning parameters in FLC can be greatly reduced. The computation load can also be alleviated for that the number of fuzzy rules is considerably decreased.

Fig. 5. The experimental scenario on the real road environment.

IV. Experimental Results

The proposed longitudinal automation system is implemented on a commercial vehicle named TAIWAN *i*TS-1, Savrian, manufactured by Mitsubishi motor company. The feedback velocity of the vehicle is measured from the wheel-velocity instrument of the front left-tire. For the headway distance measurement, one laser radar (LMS291, manufactured by SICK), is employed to the automation system by the connection through RS-232. The permissible distance of radar in forward direction is set to 80 m, however, the feasible distance in practice is 40 m. As to the angle of the scanning beam, the maximum value for radar is 50 degree in both left and right planes. It is assumed that the turning angle for the scanning beam is adaptive to be according to the algorithm derived in Section III. However, note that there is no auto-turning scheme in the function of LMS291, thus in this work, the acquired sensory distance is determined according to the measured one with the calculated expanding angle of radar. In addition, the angle sensor is installed around the axis of the steering wheel, and through CAN bus to the automation system. The whole automation is built in the real-time Microautobox (MABX), which is a compact stand-alone unit with rapid prototype of control design. The more detailed information of MABX is available at http://www.dspace.com/ww/en/pub/home/products/hw/microautob.cfm. The throttle pedal is adjusted by a DC-motor with the feedback signal of the throttle position sensor, to yield the velocity tracking for vehicle control.

To exhibit the validness of the proposed longitudinal automation system, many experiments have bee taken in the expressway (Chutung-Nanliao segment, Taiwan), in which the legal highest velocity is 90 km/h. The scenario of experiments at the real road is illustrated in Fig. 5. Initially the subject vehicle is in the automatic vehicle following mode, and maintains the safety headway distance according to the current velocity (about 75 km/h). The sampled history of experiments with the scheme of adaptive sensory processor is depicted in Fig. 6. As shown in the second graph, here the fixed headway time is set as 1 second the same, such that the desired headway distance is about 21 m. There is no missing detection of the preceding vehicle during the vehicle

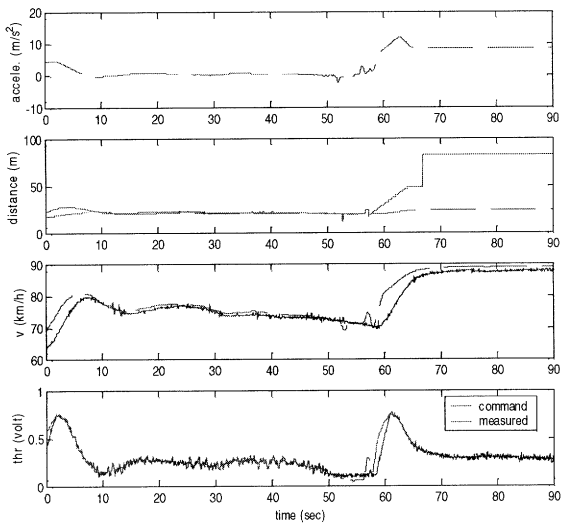

Fig. 6. The experimental scenario on the real road environment.

following control mode, and the throttle action also performs smooth, as in the bottom graph. Once the preceding vehicle changes the original lane, the subject vehicle automatically switches to the velocity cruise tracking mode and accelerates to the original desired velocity 90 km/h, as shown in the third graph. It can be seen that the steady-state throttle voltage after the acceleration is larger values for the higher velocity than the slower velocity. If one vehicle cuts in the forward direction, or radar detects the slower vehicle ahead within the feasible range (40 m), then the throttle pedal of the subject vehicle will be adjusted to follow the preceding vehicle with the safety distance according the current velocity. Besides the high velocity operation, although not shown, the operation of low velocity (20 km/h upward) can also be handled by the regulation control against gear changes and torque converter of the vehicle engine.

During these experimental tests of the longitudinal automation system, the acceleration of the subject vehicle is recorded for comfort analysis. One accelerometer is located at the center of gravity of the subject vehicle for only the longitudinal motion is of interest. In Table IV, it is clear to see that the comfort index a_w within different sampling intervals are all extremely satisfied with the constraint of no discomfort in ISO 2631 standard. The recorded acceleration data of the subject vehicle are not restricted to only one operation mode but also include the transition process. Even if the human driver acts brake too much such that the vehicle is decelerated to much lower velocity, yet the automation system performs smooth acceleration to the desired velocity under the request for comfort. Both the selections of the saturated acceleration $a_{f\max}$ and headway time σ can be adjusted from the human driver according to personal driving behavior and favor. The braking action is reserved to the human driver to take the awareness of emergency, while the concentration on maintaining a safety headway distance is delivered to the longitudinal automation system. Therefore, in addition to the comfort requirement, the workload reduction from the human driver can also be achieved.

TABLE IV
FREQUENCY-WEIGHTED ACCELERATION DURING DIFFERENT SAMPLING INTERVALS

Sampling interval (sec.)	a_w (m/s^2)
0 ~ 30	0.0522
0 ~ 40	0.0688
0 ~ 50	0.0585
0 ~ 60	0.0755

V. Conclusion and Future Works

Integration of human-in-the-loop design into a longitudinal automation design is presented in this paper, and the overall system is successfully implemented on a passenger vehicle tested in real road environments. The longitudinal automation system is composed of the adaptive sensory processor, the supervisory control, and the regulation control. The system safety is improved by inclusion of adaptive sensory scheme to prevent the missing detection of the preceding vehicle on curved roads. The supervisory control is designed to switch between different modes automatically and operate within the bound acceleration constraint without the requirement of v-v communication. Based on the reference velocity commanded from the supervisory control, the regulation control is to execute the vehicle velocity tracking through the throttle. The proposed automation system is to assist the human driver in the velocity and inter-vehicle space control such as to yield the workload reduction of driving. Finally, the experimental results at real roads verify the validness of the longitudinal automation system. Furthermore, the ride comfort is also achieved through the examination of the standard ISO 2631.

Acknowledgment

This work is supported by the program of Promoting Academic Excellence of Universities under Grant. No. 91X104 EX-91-E-FA06-4-4. We also thank Tseng-Wei Chang and Tien-Yu Liao for the cooperation of hardware work.

References

[1] H. Raza and P. Ioannou, "Vehicle following control design for automated highway systems," *IEEE Trans. Contr. Syst.*, pp. 43-60, Dec. 1996.

[2] R. Rajamani et al., "Design and experimental implementation of longitudinal control for a platoon of automated vehicles," *Trans. ASME J. Dyn. Syst. Meas. Contr.*, vol. 122, pp. 470-476, Sep. 2000.

[3] J. E. Naranjo et al., "Adaptive fuzzy control for inter-vehicle gap keeping," *IEEE Trans. Intell. Transport. Syst.*, vol. 4, no. 3, pp. 132-142, Sep. 2003.

[4] A. Vahidi and A. Eskandarian, "Research advances in intelligent collision avoidance and adaptive cruise control," *IEEE Trans. Intell. Transport. Syst.*, vol. 4, no. 3, pp. 143-153, Sep. 2003.

[5] "ISO 2631/1: Mechanical Vibration and Shock-Evaluation of Human Exposure to Whole-body Vibration, Part 1. General Requirements," 1997.

[6] S. J. Wu et al., "The automated lane-keeping design for an intelligent vehicle," in *Proc. Intell. Veh. Symp.* 2005, Las Vegas, 2005, pp. 508-513.

[7] B. J. Choi, S. W. Kwak, and B. K. Kim, "Design stability analysis of single-input fuzzy logic controller," *IEEE Trans. Syst. Man, and Cyber. B*, vol. 30, no. 2, pp. 303-309, April 2000.